Structural, optical, and electrical properties of ZnO nanofilms deposited over PS substrate

Reza Shabannia[1] ✉, *Abbas Mohammed Selman*[2]

[1]*Department of Physics, College of Science, Babol University of Technology, Babol, Iran*
[2]*Department of Pharmacognosy and Medicinal Plants, Faculty of Pharmacy, University of Kufa, Najaf, Iraq*
✉ *E-mail: rezash56rami@gmail.com*

Published in Micro & Nano Letters; Received on 21st December 2016; Revised on 14th February 2017; Accepted on 17th February 2017

The research successfully revealed the fabrication of zinc oxide (ZnO) nanofilms with hexagonal (002) structure grown on porous silicon (PS) substrate using chemical bath deposition method. Their structural, optical, and electric characteristics were investigated through X-ray diffraction, field emission scanning electron microscopy (FESEM), and photoluminescence spectroscopy. FESEM showed that ZnO nanofilms were formed on top and inside the pores of PS substrate with hexagonal shape. The strong ultraviolet emission of ZnO nanofilms is also presented at ~383 nm near the band edge energy levels which can be applied in semiconductor device both photoelectron devices and chemical sensors. In addition, current–voltage (*I–V*) characteristics revealed that the current level for ZnO nanofilms was about three times larger than for PS layer.

1. Introduction: Among semiconductor materials, zinc oxide (ZnO) nanostructures with extraordinary electronic, optical, and chemical properties have encouraged many researchers to develop novel electronic and optoelectronic devices such as ultraviolet (UV) photodetectors, gas sensor, light-emitting diodes, and solar cells [1–6]. Therefore, detailed understanding on the electrical and optical properties of ZnO nanostructures is of major importance to be utilised in the optoelectronics industry because the electronic and optoelectronic characteristics of ZnO nanostructures strongly depend on carrier relaxation processes. To date, various methods have been utilised to synthesise ZnO nanostructures on diverse substrate types [7–10]. The morphology and nature of fabricated ZnO nanostructures can be controlled by significant factors such as surface morphology and structure of substrates as well as their lattice mismatch with ZnO nanostructures. High-quality ZnO nanostructures directly grow or deposit on silicon (Si) substrate is difficult, because there is a large stress between ZnO and Si substrates due to the mismatch in their thermal expansion coefficients and lattice constants [11]. Therefore, it is necessary to look for a better substrate for growing high-quality ZnO nanostructure. In recent years, much effort has been made to overcome these problems by the use of compliant layers such as porous semiconductor intermediate layer [12]. Since the past few decades, the porous Si (PS) substrates have attracted significant interests toward applying it in developing Si-based optoelectronic devices due to its strong absorbability, adjustable roughness, high-temperature resistant, large internal surface, and low cost [13, 14]. The PS layer reduces the large mismatches in the lattice constants and thermal expansion coefficients between the ZnO and Si substrates, which also reduces the large stress between the ZnO nanostructures and Si substrate [15]. Salman *et al.* [16] deposited nanocrystalline ZnO film by using radio-frequency sputtering system on PS substrate. Recently, various kinds and varied morphologies of nanostructured semiconductor materials with high crystallinity, optical, and electrical properties have been fabricated using chemical bath deposition (CBD) [17–20].

In the present work, nanosized pores were created in an n-type Si (100) substrate by photoelectrochemical etching. The ZnO nanoparticles were fabricated by CBD method on a PS substrate at low temperature. This process is simple and uses low-cost instruments compared with other wet chemical processes. The structural, optical, and electrical characteristics of the ZnO nanofilms grown on a PS substrate were investigated.

2. Experimental results: The first step is creating the porous structure on an n-type Si(100) substrate using the photoelectrochemical etching method [21, 22]. The PS layer was formed by the photoelectrochemical etching process in a teflon cell, which is a mixture of hydrofluoric acid and 96% ethanol combined using a volume ratio of 1:4. In this process, an inert platinum wire and the Si substrate were used as the cathode and anode, respectively. The etching process was carried out with a constant current density of 20 mA/cm^2 for 15 min. The PS samples were washed with deionised (DI) water and dried using nitrogen gas. After that, the second step was carried out by coating a 50 nm thick ZnO thin film on the prepared PS surface via a radio-frequency magnetron sputtering system. The ZnO nanofilms were subsequently produced by vertically immersing the ZnO seeded PS substrate into a chemical bath containing an aqueous solution of 0.1 mol/l zinc nitrate hexahydrate and an equal molar concentration of hexamethylenetetramine, which were dissolved in DI water at 80°C, respectively. The growth temperature and period were fixed to 80°C and 2.5 h, respectively.

The field emission scanning electron microscopy (FESEM) (Field Electron and Ion (FEI). 'The FEI company was founded in 1971 as Field Electron and Ion Co.'/Nova NanoSEM 450) was used to study the surface morphology of ZnO nanofilms. The X-ray diffraction (XRD) (Panalytical X'Pert Pro MRD PW3040: 'Probe (Pro)' and 'Materials Research Diffractometers (MRD)' PW3040) was employed to study the structure and orientation of ZnO nanofilms. The optical property of ZnO nanofilms was investigated by photoluminescence (PL) spectroscopy (Jobin Yvon High Resolution (HR) 800 UV, Edison, NJ, USA) at room temperature. The current–voltage (*I–V*) characteristics of the ZnO nanofilms were performed with the increasing step of applied voltage 0.01 V within the voltage ranging from −5.0 to +5.0 V using a computer-controlled integrated source meter (Keithley 2400) at room temperature.

3. Results and discussion: Fig. 1*a* displays the random distribution of pores on the PS substrate. The porosity was measured using the weighing method, as shown by the following equation [23]

$$P(\%) = \frac{m_1 - m_2}{m_1 - m_3} \times 100\% \quad (1)$$

doi: 10.1049/mnl.2016.0753

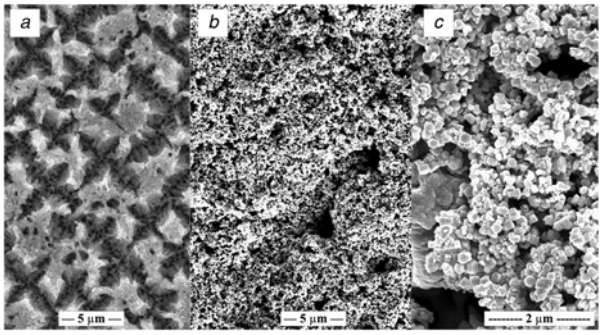

Fig. 1 *FESEM images of*
a PS substrate
b Low magnification of ZnO nanofilms grown on PS substrate
c High magnification of ZnO nanofilms grown on PS substrate

where m_1, m_2, and m_3 are before the start of the etching process, after the porous layer was formed, and after the porous layer was removed by dipping the sample in potassium hydroxide solution, respectively. The porosity percentages of the *n*-PS (100) layer were 56%. Meanwhile, Figs. 1*b* and *c* demonstrate low and high magnifications of the fabricated ZnO nanofilms surface morphology grown on the PS substrate, respectively. It can be seen that the FESEM images have demonstrated high-density ZnO nanofilms distributed over the entire PS substrate surface. Furthermore, Fig. 1*b* displayed the ZnO nanofilms formed on top and inside the pores of PS substrate with hexagonal shape with their diameters varied from 20 to 100 nm. The thickness of the ZnO nanofilms is <70 nm, mostly between 30 and 50 nm. These fabricated ZnO nanofilms on PS substrate can be very useful in applications including photodetection and gas sensors devices.

The XRD measurement was applied to obtain the crystalline orientation and structure of the ZnO nanofilms. The XRD spectrum measured from the ZnO nanofilms fabricated on the PS substrate is shown in Fig. 2. All XRD patterns have matched the wurtzite hexagonal phase of the standard data for ZnO (The Inorganic Crystal Structure Database (ICSD) (for inorganic compounds) 01-074-0534). Moreover, the peaks in Fig. 2 indicate the presence of (100), (002), and (101) planes of ZnO material. The high-intensity (002) peak in the XRD pattern compared with (100) and (101) peaks suggested that ZnO nanofilms prefer to grow in the (002) orientation because the free energy per unit area of (002) orientation is lowest in the ZnO crystal [24]. The grain size of the ZnO nanofilms along the (002) peak is obtained by the following Scherrer equation [25]

$$D = \frac{0.9\lambda}{\beta \cos \theta} \tag{2}$$

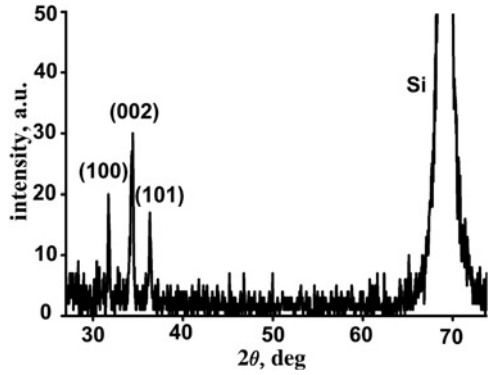

Fig. 2 *Typical XRD pattern of ZnO nanofilms grown on PS substrate*

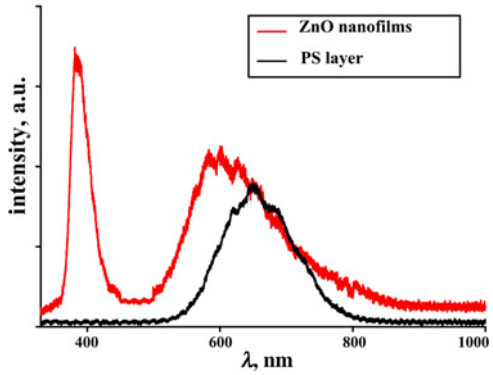

Fig. 3 *PL spectra of ZnO nanofilms and PS layer*

where D, θ, λ, and β represent the average crystallite size, Bragg diffraction angle, X-ray radiation wavelength, and full width at half maximum value, respectively. The grain size of ZnO nanofilms grown on PS substrate along the (002) peak was 30.4 nm. The strain of the ZnO nanofilms synthesised on the PS substrate along the *c*-axis was obtained by using the following equation [26]

$$\varepsilon_{zz} = \frac{c - c_0}{c_0} \times 100 \tag{3}$$

where c and c_0 are the lattice constants of the ZnO nanofilms obtained from the XRD data and the standard lattice constant for unstrained ZnO, respectively. The compressive strain of ZnO nanofilms was −0.0153%.

Fig. 3 displays the PL spectra of ZnO nanofilms and PS substrate. It was observed that the high-intensity emission peak is located at 643 nm in the PL spectrum of PS layer, which indicates the superior quality of the PS layer [26]. Additionally, the PL spectrum of ZnO nanofilms displayed sharp near band edge emission (NBE) at ∼383 nm that can be ascribed to the recombination of electron–hole NBE energy levels [27]. The strong and broad visible emission of ZnO nanofilms is attributed to the PS layer and intrinsic defects in ZnO such as oxygen and zinc vacancies [28]. The comparison between high and sharp intensity of UV emission and low intensity of visible emission demonstrated a high optical quality of ZnO nanofilms. The strong UV emission of ZnO nanofilms is also presented at ∼383 nm near the band edge energy levels which can be applied in semiconductor device both photoelectron devices and chemical sensors.

Fig. 4 demonstrates the typical *I–V* property of PS substrate and ZnO nanofilms by changing the bias voltage from −5 to +5 V at room temperature under ambient condition. Using the bias voltage of +5 V, the current level of the PS substrate and ZnO nanofilms was observed to have reached 340 and 990 μA, respectively.

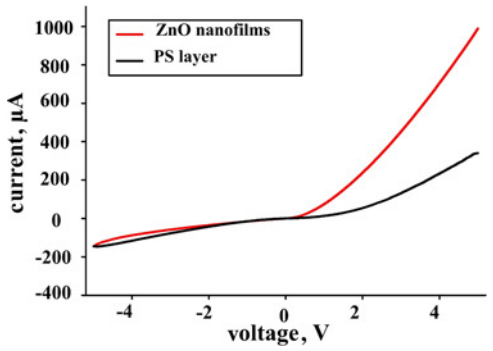

Fig. 4 *Current–voltage characteristics of the PS substrate and ZnO nanofilms*

In the ambient condition, the resistance of PS layer was 14.7 kΩ, whereas the ZnO nanofilms resistance was 5 kΩ with a 5 V bias voltage. The decrease in ZnO nanofilms resistance was due to the contribution from the photocurrent generation. The photogenerated charges produced under the effect of the applied electric field led to a photocurrent that was added to the bias current, effectively increasing the conductivity of the device [29]. In addition, Fig. 4 reveals that the measured current level for ZnO nanofilms was about three times larger than for PS layer. The increase in photocurrent could be attributed to the mobility and lifetime of photocarriers and the large surface-area-to-volume of ZnO nanofilms.

4. Conclusions: ZnO nanofilms were successfully fabricated on a PS substrate using the CBD method. FESEM images confirmed that the hexagonal shaped ZnO nanofilms are formed on top and inside the pores of the PS substrate. The diameter of ZnO nanofilms were varied from 20 to 100 nm. The PL spectrum of ZnO nanofilms exhibited sharp NBE and broad green–red emissions at ∼383 nm and 500–700 nm, respectively. *I–V* characteristics revealed that the photocurrent for ZnO nanofilms was about three times larger than for PS layer. This further concluded that the synthesis of ZnO nanofilms with high density can be very useful for chemical sensors, photovoltaics, and photocatalysis.

5. Acknowledgment: The authors gratefully acknowledge the financial support of Babol University of Technology.

6 References

[1] Hosseini Z., Mortezaali A.: 'Room temperature H_2S gas sensor based on rather aligned ZnO nanorods with flower-like structures', *Sens. Actuators B, Chem.*, 2015, **207**, pp. 865–871
[2] Shabannia R., Hassan H.A.: 'Characteristics of photoconductive UV photodetector based on ZnO nanorods grown on polyethylene naphthalate substrate by chemical bath deposition method', *Electron. Mater. Lett.*, 2014, **10**, pp. 837–843
[3] Gurav K., Gang M., Shin S., *ET AL.*: 'Gas sensing properties of hydrothermally grown ZnO nanorods with different aspect ratios', *Sens. Actuators B, Chem.*, 2014, **190**, pp. 439–445
[4] Echresh A., Chey C.O., Shoushtari M.Z., *ET AL.*: 'Tuning the emission of ZnO nanorods based light emitting diodes using Ag doping', *J. Appl. Phys.*, 2014, **116**, p. 193104
[5] Thambidurai M., Muthukumarasamy N., Velauthapillai D., *ET AL.*: 'Synthesis of garland like ZnO nanorods and their application in dye sensitized solar cells', *Mater. Lett.*, 2013, **92**, pp. 104–107
[6] Gonzalez-Valls I., Yu Y., Ballesteros B., *ET AL.*: 'Synthesis conditions, light intensity and temperature effect on the performance of ZnO nanorods-based dye sensitized solar cells', *J. Power Sources*, 2011, **196**, pp. 6609–6621
[7] Hassan J., Mahdi M., Chin C., *ET AL.*: 'Room temperature hydrogen gas sensor based on ZnO nanorod arrays grown on a SiO_2/Si substrate via a microwave-assisted chemical solution method', *J. Alloys Compd.*, 2013, **546**, pp. 107–111
[8] Hassan J., Mahdi M., Chin C., *ET AL.*: 'Room-temperature hydrogen gas sensor with ZnO nanorod arrays grown on a quartz substrate', *Phys. E, Low-dimens. Syst. Nanostruct.*, 2012, **46**, pp. 254–258
[9] Shabannia R., Hassan H.A.: 'Controllable vertically aligned ZnO nanorods on flexible polyethylene naphthalate (PEN) substrate using chemical bath deposition synthesis', *Appl. Phys. A*, 2014, **114**, pp. 579–584
[10] Hsu C.-L., Gao Y.-D., Chen Y.-S., *ET AL.*: 'Vertical Ti doped ZnO nanorods based on ethanol gas sensor prepared on glass by furnace system with hotwire assistance', *Sens. Actuators B, Chem.*, 2014, **192**, pp. 550–557
[11] Chu S., Olmedo M., Yang Z., *ET AL.*: 'Electrically pumped ultraviolet ZnO diode lasers on Si', *Appl. Phys. Lett.*, 2008, **93**, p. 181106
[12] Rai P., Song H.-M., Kim Y.-S., *ET AL.*: 'Microwave assisted hydrothermal synthesis of single crystalline ZnO nanorods for gas sensor application', *Mater. Lett.*, 2012, **68**, pp. 90–93
[13] Chuah L.S., Hassan Z., Ng S.S., *ET AL.*: 'Porous Si(111) and Si(100) as an intermediate buffer layer for nanocrystalline InN films', *J. Alloys Compd.*, 2009, **479**, pp. L54–L58
[14] Shaoqiang C., Jian Z., Xiao F., *ET AL.*: 'Nanocrystalline ZnO thin films on porous silicon/silicon substrates obtained by sol–gel technique', *Appl. Surf. Sci.*, 2005, **241**, pp. 384–391
[15] Chen J.Y., Sun K.W.: 'Growth of vertically aligned ZnO nanorod arrays as antireflection layer on silicon solar cells', *Sol. Energy Mater. Sol. Cells*, 2010, **94**, pp. 930–934
[16] Salman K.A., Omar K., Hassan Z.: 'Nanocrystalline ZnO film grown on porous silicon layer by radio frequency sputtering system', *Mater. Lett.*, 2012, **68**, pp. 51–53
[17] Selman A.M., Hassan Z.: 'Growth and characterization of rutile TiO_2 nanorods on various substrates with fabricated fast-response metal–semiconductor–metal UV detector based on Si substrate', *Superlattices Microstruct.*, 2015, **83**, pp. 549–564
[18] Husham M., Hassan Z., Mahdi M., *ET AL.*: 'Fabrication and characterization of nanocrystalline CdS thin film-based optical sensor grown via microwave-assisted chemical bath deposition', *Superlattices Microstruct.*, 2014, **67**, pp. 8–16
[19] Hassan J., Mahdi M., Ramizy A., *ET AL.*: 'Fabrication and characterization of ZnO nanorods/p-6H–SiC heterojunction LED by microwave-assisted chemical bath deposition', *Superlattices Microstruct.*, 2013, **53**, pp. 31–38
[20] Shabannia R.: 'Fabrication and characterization of flower-like ZnO nanostructures grown chemically on flexible PEN substrate', *Micro Nano Lett.*, 2016, **11**, (8), pp. 457–459
[21] Shabannia R.: 'Vertically aligned ZnO nanorods on porous silicon substrates: effect of growth time', *Prog. Nat. Sci., Mater. Int.*, 2015, **25**, (2), pp. 95–100
[22] Shabannia R.: 'Effect of annealing temperature on the structural, optical and electrical properties of ZnO thin films grown chemically on PS substrate', *J. Mater. Sci., Mater. Electron.*, 2016, **27**, pp. 6413–6418
[23] Bisi O., Ossicini S., Pavesi L.: 'Porous silicon: a quantum sponge structure for silicon based optoelectronics', *Surf. Sci. Rep.*, 2000, **38**, pp. 1–126
[24] Lee J., Gao W., Li Z., *ET AL.*: 'Sputtered deposited nanocrystalline ZnO films: a correlation between electrical, optical and microstructural properties', *Appl. Phys. A, Mater. Sci. Process.*, 2005, **80**, pp. 1641–1646
[25] Sanon G., Rup R., Mansingh A.: 'Growth and characterization of tin oxide films prepared by chemical vapour deposition', *Thin Solid Films*, 1990, **190**, pp. 287–301
[26] Shabannia R., Abu Hassan H.: 'Growth and characterization of aligned ZnO nanorods synthesized on porous silicon', *Mater. Lett.*, 2013, **98**, pp. 135–137
[27] Abdulgafour H., Yam F., Hassan Z., *ET AL.*: 'ZnO nanocoral reef grown on porous silicon substrates without catalyst', *J. Alloys Compd.*, 2011, **509**, pp. 5627–5630
[28] Shabannia R., Hassan H.A.: 'Growth and characterization of vertically aligned ZnO nanorods grown on porous silicon: effect of precursor concentration', *Superlattices Microstruct.*, 2013, **62**, pp. 242–250
[29] Abdulgafour H., Hassan Z., Ahmed N., *ET AL.*: 'Comparative study of ultraviolet detectors based on ZnO nanostructures grown on different substrates', *J. Appl. Phys.*, 2012, **112**, p. 074510

doi: 10.1049/mnl.2016.0753